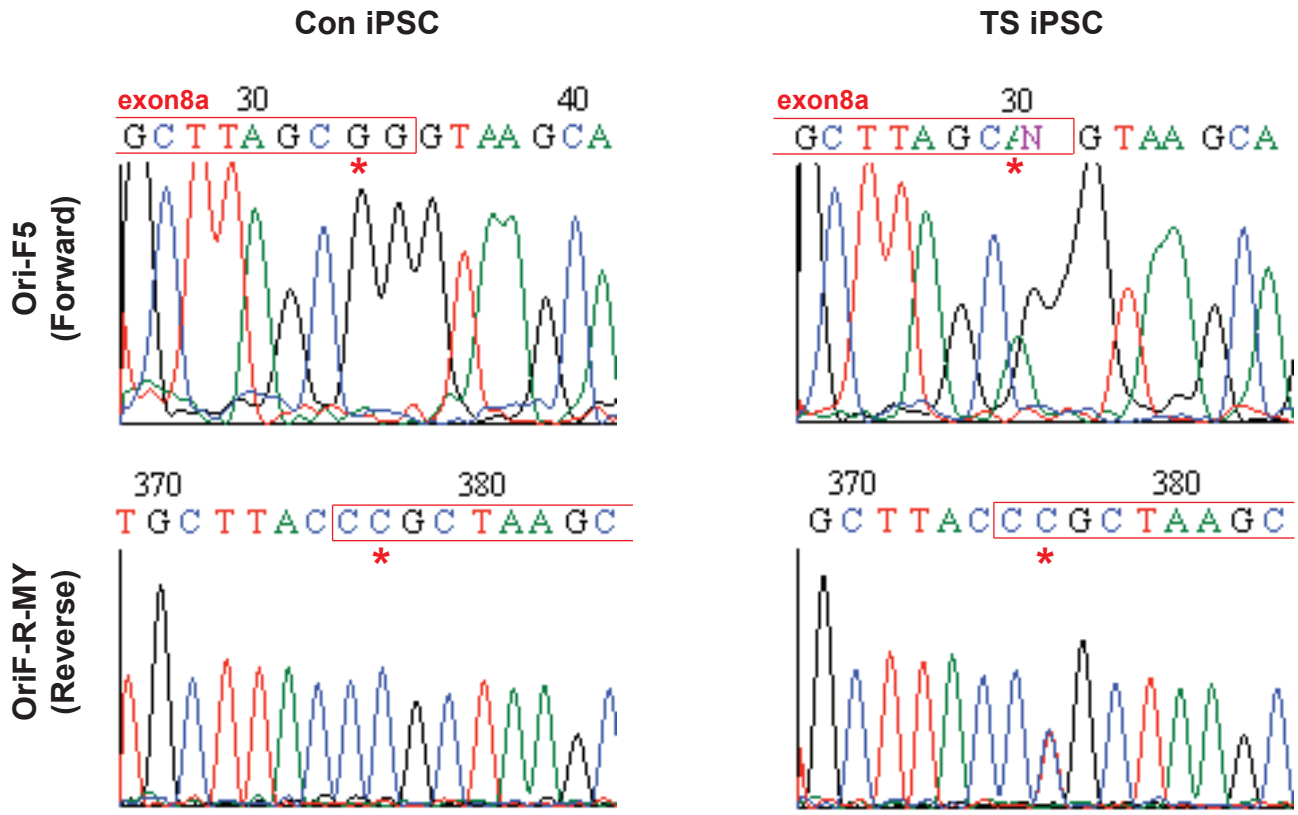

Supplementary Figure 1. Sequencing of genomic DNA from control and TS iPSCs to confirm TS mutation in exon8a. Sequence results of genomic DNA from control (left) and TS iPSCs (right). The G1216A mutation is indicated by the red asterisk and the boundary of exon 8a is shown by the red boxes.

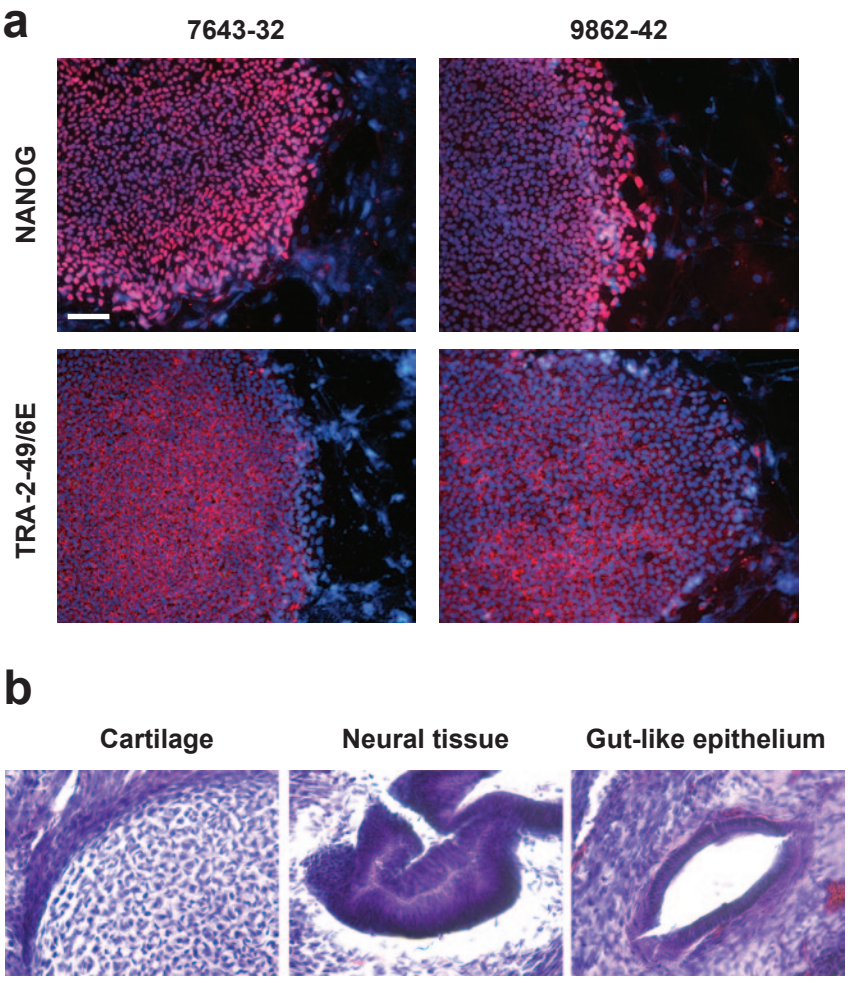

Supplementary Figure 2. iPSC immunocytochemistry and teratoma formation assay
a) Immunocytochemistry of iPSCs generated from two patients (clone, 7643-32 and 9862-42) using antibodies that recognize the pluripotency markers, NANOG (top, red) and TRA-2-49/6E (bottom, red). Hoechst staining (blue) indicates the nuclei. Scale bar is 50 μm. b) Sections of a teratoma formed by TS iPSCs (clone, 7643-7) stained with hematoxylin and eosin. Tissue derived from the three germ layers such as cartilage (left, mesoderm), neural tissue (middle, ectoderm) and gut-like epithelium (right, endoderm) could be detected and were observed in all control and TS iPSCs (Supplementary Table1).

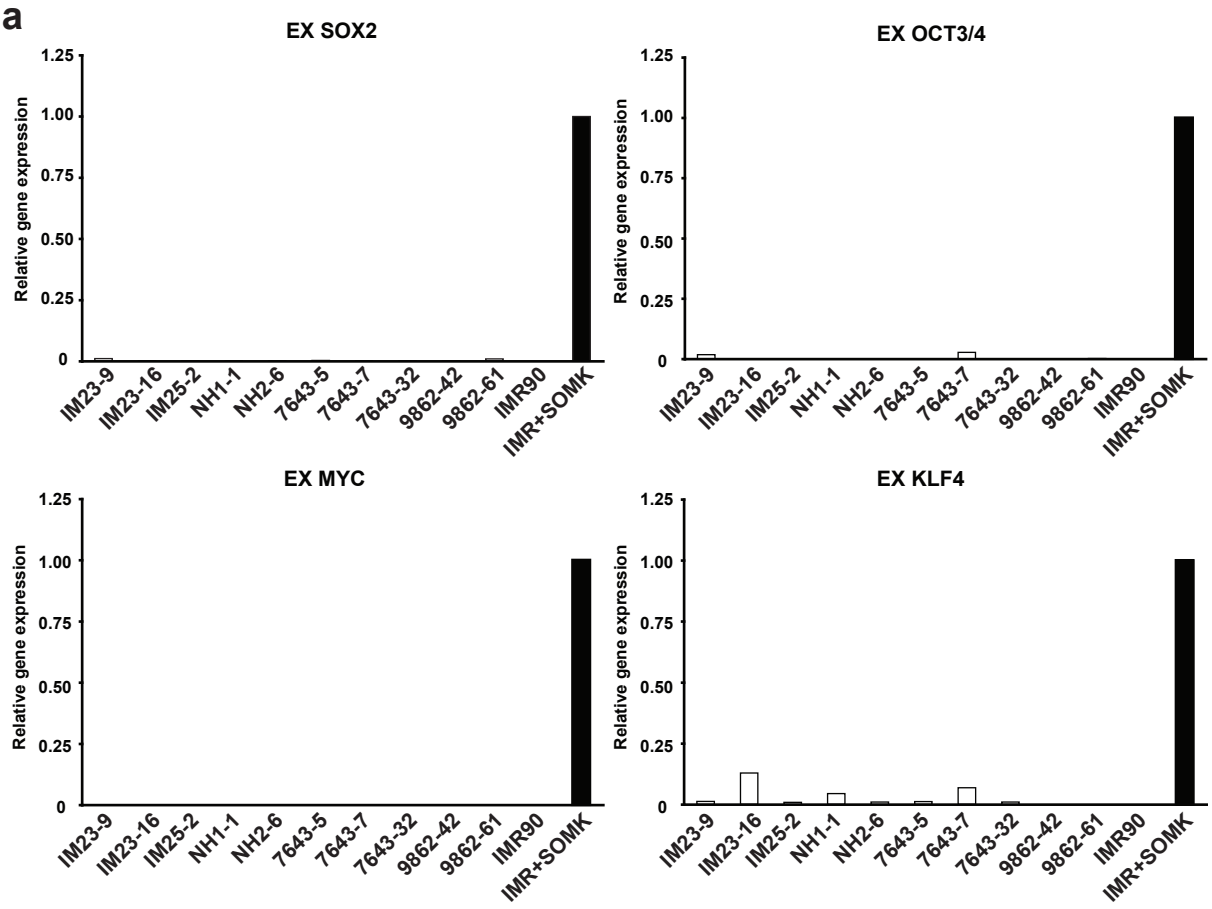

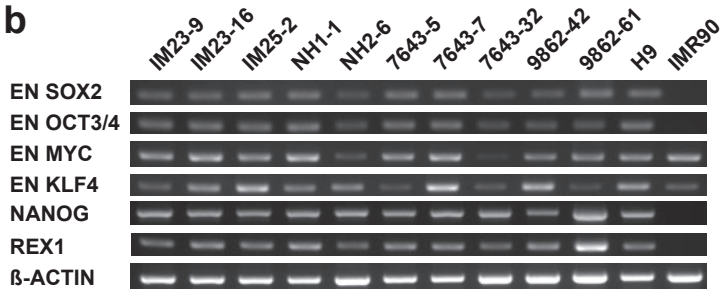

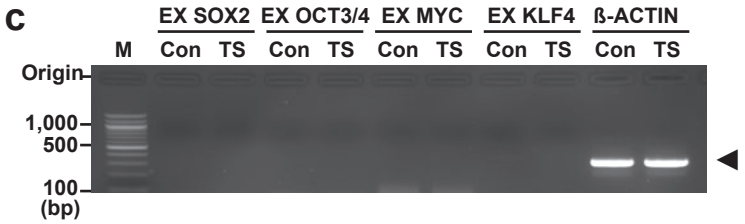

Supplementary Figure 3. Gene expression profiling of iPSCs a) Quantitative RT-PCR analysis of the expression of reprograming genes in TS and control iPSC lines. IMR90 are human fibroblasts that were used as a control. IMR+SOMK are IMR90 cells infected with the four retroviruses (SOX2, OCT3/4, C-MYC and KLF4) used for reprograming. The expression of exogenous (EX) genes was normalized relative to GAPDH. b) Semi-quantitative RT-PCR analysis of endogenous gene expression in the iPSC lines used in the study. The expression of endogenous (EN) SOX2, OCT3/4, C-MYC and KLF4 was examined as well as the pluripotent markers NANOG and REX1 and house keeping gene β-ACTIN (see Supplementary Table 2 for primer sequences). Human embryonic stem cell line H9 and human fibroblasts IMR90 were used as control samples. c) Conventional RT-PCR was used to examine if the reprograming genes were active in cardiac cells generated from control (NH1-1) and TS iPSC lines (7643-5) at d37.

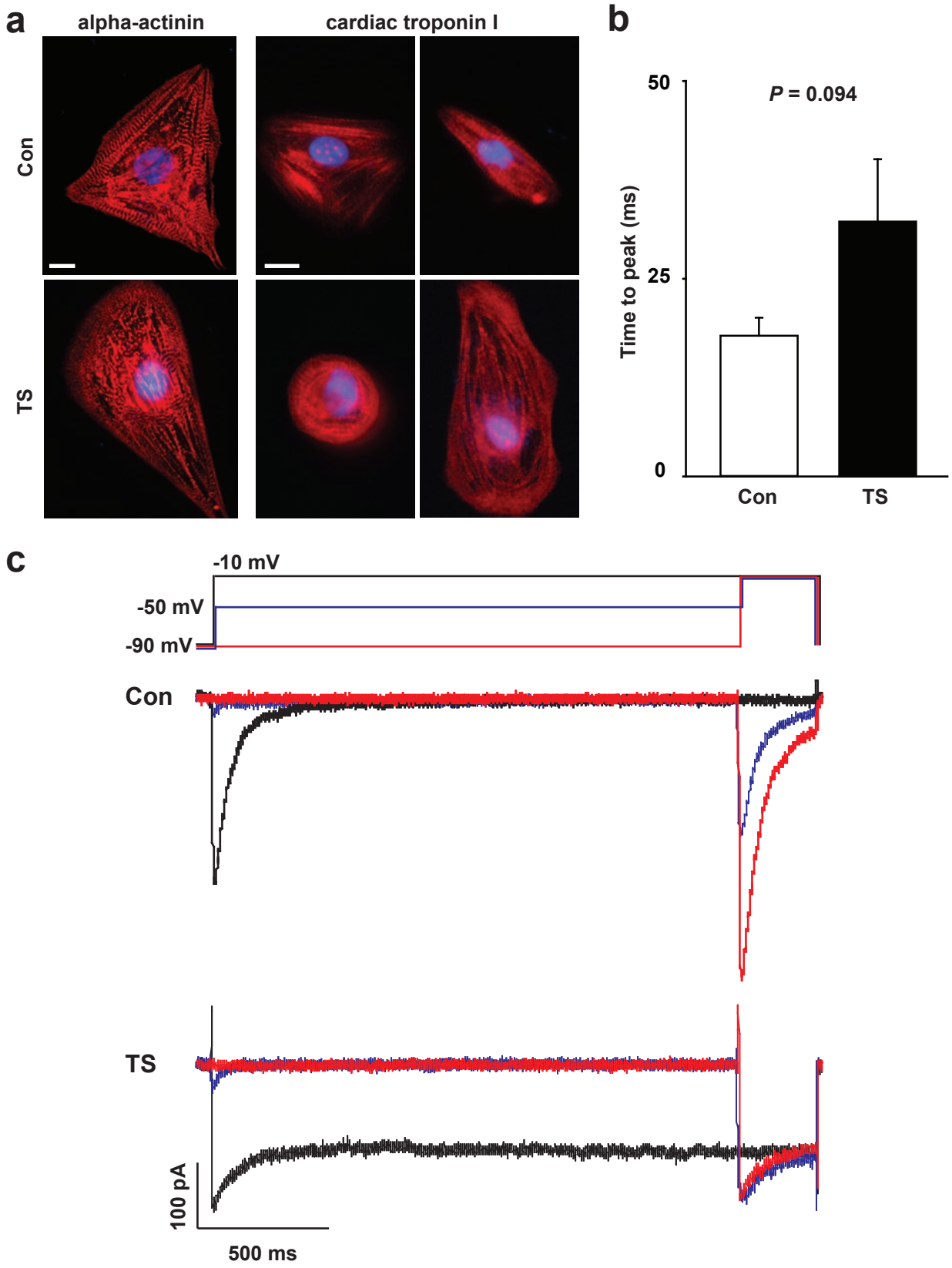

Supplementary Figure 4. Immunocytochemistry and electrophysiology of TS and control cardiomyocytes
a) Staining of human cardiomyocytes generated from control (top, NH1-1 and NH2-6) and TS iPSCs (bottom, 7643-5 and 7643-32) using antibodies against α-Actinin (left, see Fig 2a) and cardiac Troponin I (right). Scale bar, 10 μm. b) Time to the peak of the Ba2+ current in TS and control CMs stimulated with a depolarizing pulse to -10 mV (see Fig 2b, control, *n*=23 cells in 4 lines; TS, *n*=19 in 4 lines, mean ± s.e.m, students T test). TS channels activate more slowly than WT channels. c) Representative traces of Ba2+ currents in TS and control CMs stimulated with a prepulse to -90, -50 and -10, red, blue and black traces respectively, and a test pulse to -10 mV. This pulse protocol was used to measure residual current in Fig 2e.

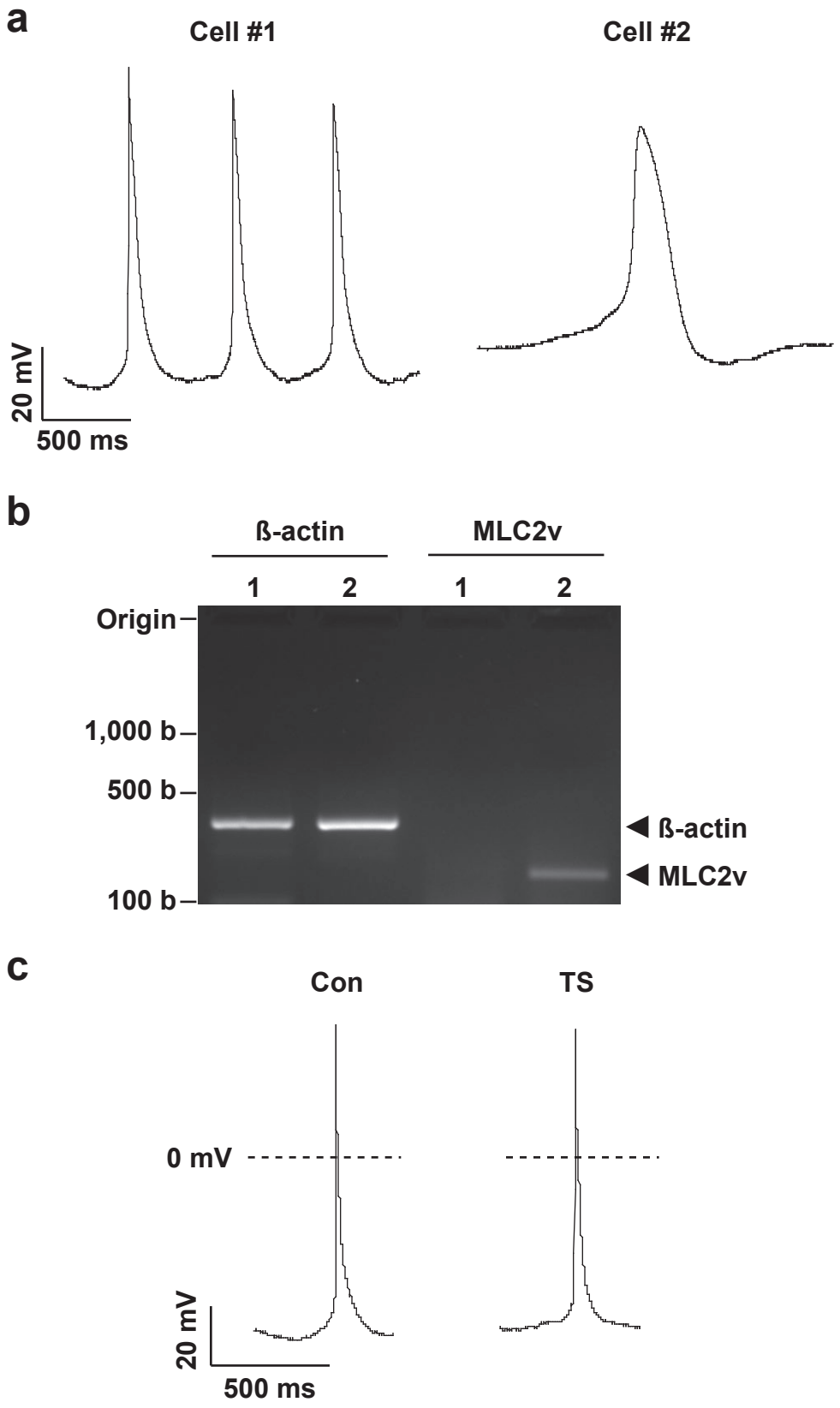

Supplementary Figure 5. Patch clamp recordings and single-cell RT-PCR of atrial and ventricular cells derived from control and TS patients a) Action potential recording of iPSC-derived atrial and ventricular cardiomyocytes. b) Agarose gel electrophoresis of single cell RT-PCR products showing expression of the ventricular marker MLC2v in cell #2 but not in cell #1. β-actin was expressed in both cells. c) Recording of action potentials in atrial cells from control (left) and TS (right) CMs did not reveal any significant differences.

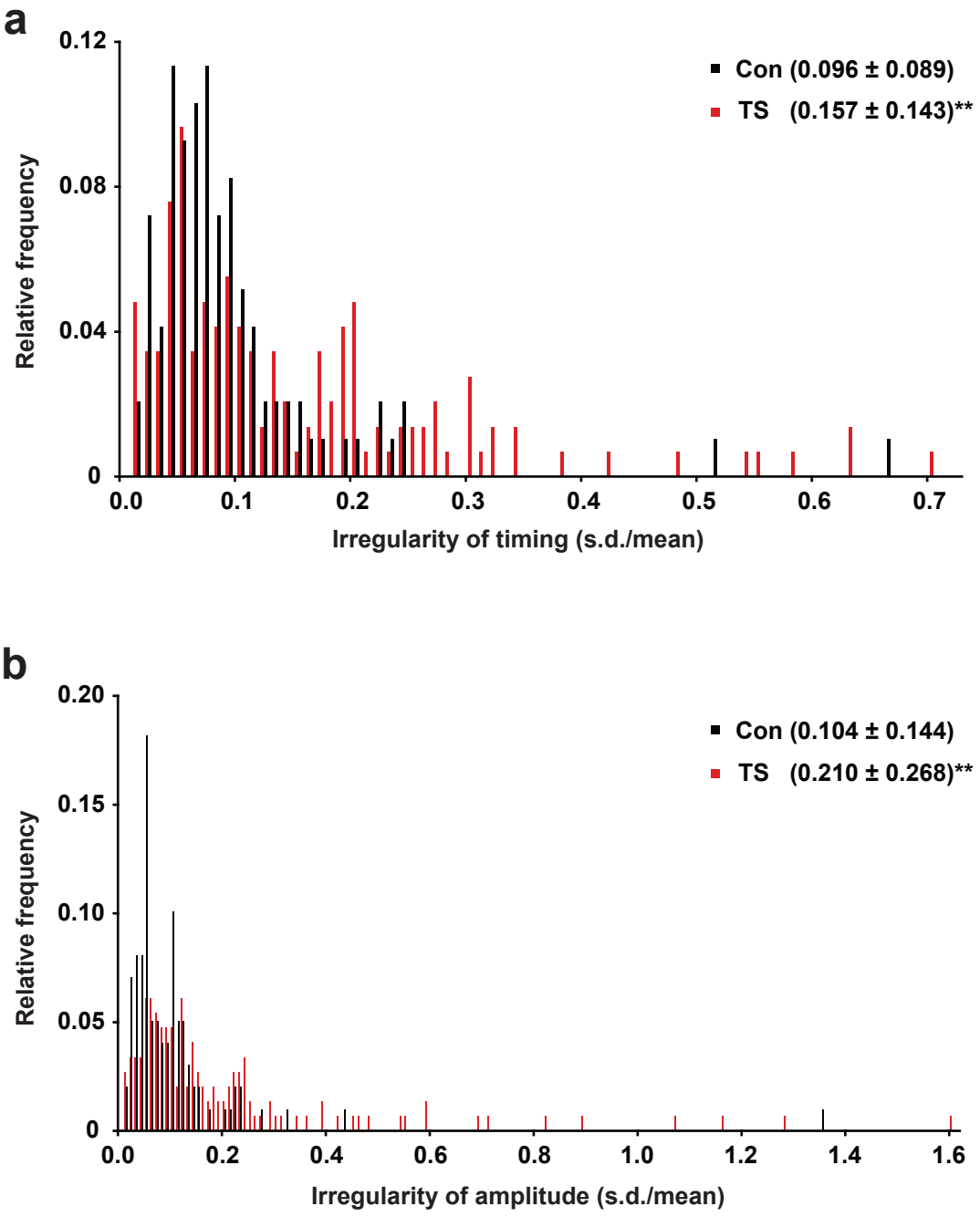

Supplementary Figure 6. Irregularity of spontaneous Ca2+ transients in TS cardiomyocytes Histogram showing the proportion of cells with Ca2+ transients of irregular frequency (a) or amplitude (b). The regularity of the contractions was calculated by dividing the standard deviation of the oscillation period by the mean of the period or by standard deviation of the amplitude by the mean of the amplitude. TS CMs were significantly more likely to have contractions with irregular frequencies and amplitudes than the controls (control, n=102 cells in 4 lines; TS, n=149 in 4 lines, mean ± s.d. **P<0.01, Students T-test).

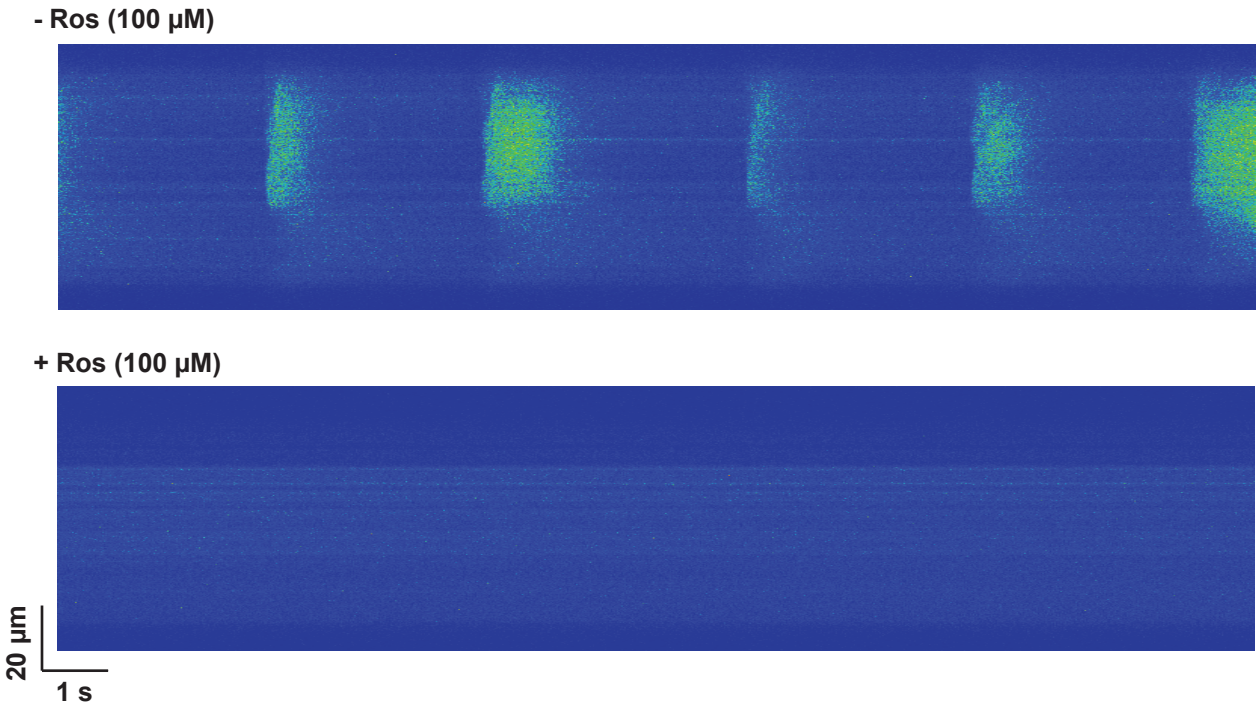

Supplementary Figure 7. Optimization of the concentration of roscovitine in TS cardiomyocytes
Line-scan images of spontaneous Ca2+ transients from TS CMs showing the irregular timing and amplitude of the Ca2+ transients (upper panel). Addition of 100 μM Ros eliminated spontaneous contractions and Ca2+ transients (lower panel, *n*=3 cells, 1 lines). A lower concentration of Ros (10 μM) didn't have significant effect on irregularity of spontaneous Ca2+ transients in TS CMs (data not shown).

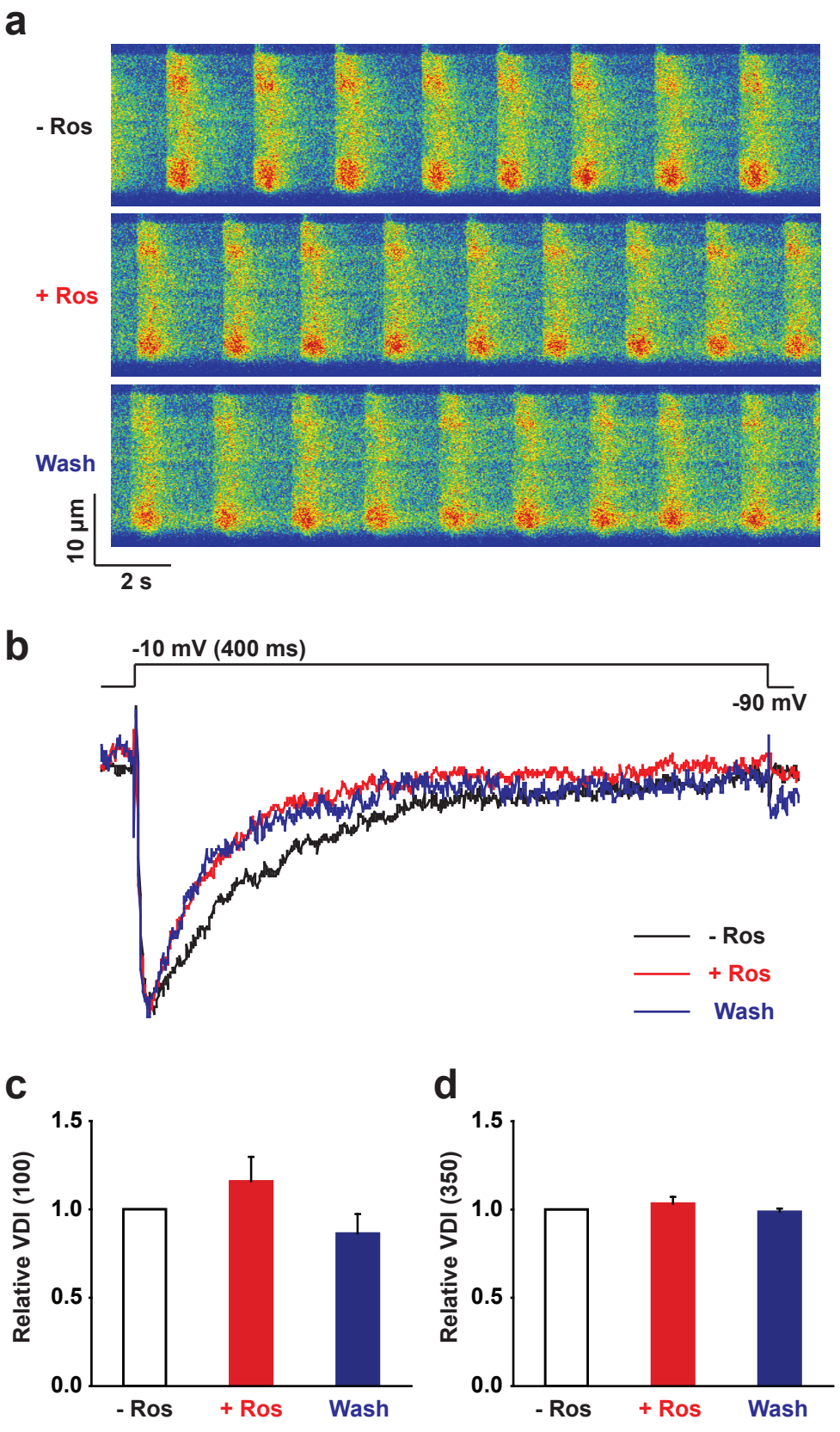

Supplementary Figure 8. Effects of Roscovitin on control CMs a) Line-scan images of spontaneous Ca2+ transients in control CMs showing the regular timing and amplitude of the Ca2+ transients. 33.3 µM Ros had no effect on the spontaneous Ca2+ transients (*n*=10 cells in 1 lines). b) Traces of Ba2+ current in control CMs show normal inactivation kinetics and no significant effect of Ros on VDI at 100 ms (c) or at 350 ms (d) (*n*=5 cells in 1 line).

Supplementary Table 1 Characterization of control and TS iPSC lines used for *in vitro* differentiation

	line	Putative viral integration site				Immunocytochemistry		Teratoma formation assay	Karyotype
		SOX2	OCT3/4	KLF4	C-MYC	NANOG	TRA-2-49/6E		
Con	IM23-9	chr22q11.2 (25087178-)	chr7p11.2 (55196937-)	chr22q12.1 (28943374-)	chr10p11.21 (21981935-)	+	+	+	+
Con	IM23-16	chr11q13.4 (71990848-)	chr7q33 (137673483+) chr16q23.2 (82100840-)	chr3q21.3 (128944884-)	chr1p13.3 (1093736535+) chr20q13.13 (48788953-)	+	+	+	+
Con	IM25-2	chr1p31 (77790178+)	chr11q13.4 (71880060-)	chr3p12.3 (79079948-) chr17q21.31 (42624647-)	chr7p14.1 (42379186+)	+	+	+	ND[2]
Con	NH1-1	chr1q42.1-43 (234747067-)	chr10q21.2 (63841589-)	chr3q27.1 (183414900-)	chr5q33.1 (150532700+)	+	+	+	+
Con	NH2-6	chr11p15.4 (2912871-)	chr15q15.1 (41047296-)	chr1q25.3 (181103951+) chr4q22.1 (89884470-)	chr3p22.3 (34048914-) chr10q26.13 (124051763+)	+	+	+	+
TS	7643-5	chr12p13.31 (8185310-)	chr4q28.1 (125861955-)	chr11p15.4 (8703661+)	chr11q13.4 (73024636+)	+	+	+	+
TS	7643-7	chr2q35 (219421964+)	ch2q32.2 (196978607+) chr13q34 (111012751-)	chr12p13.31 (6446368+)	chr12q13.3 (57850623-)	+	+	+	+
TS	7643-32	chr1q32.1 (204385326-) chr9q32(117657021-)	chr10p12.2 (23727624+)	ND[1]	chr1p32.1 (60501593-) chr7q32.3 (131286774+)	+	+	+	+
TS	9862-42	chr7q31.1 (107670711+)	chr6q22.1 (117828633-)	chr2q31.1 (176979044+)	chr1p34.3 (36912928) chr20p13 (3868985+)	+	+	+	+
TS	9862-61	chr1p34.3 (36817536-)	chr12q13.13 (52213638-)	chr8p23.2 (5024317+)	chr5q35.1 (172226554-)	+	+	+	+

ND[1], not determined because reliable PCR products were not obtained; ND[2], not determined yet

Supplementary Table 2. Primer Sequences

Primer	Sequence (5` to 3`)	Applications
pMXs-AS3200	TTATCGTCGACCACTGTGCTGCTG	RT-PCR, exogenous genes in iPSCs
Nanog-S968	CAGCCCCGATTCTTCCACCAGTCCC	RT-PCR, endogenous Nanog
Nanog-AS1334	CGGAAGATTCCCAGTCGGGTTCACC	RT-PCR, endogenous Nanog
Rex1-F	CAGATCCTAAACAGCTCGCAGAAT	RT-PCR, endogenous Rex1
Rex1-R	GCGTACGCAAATTAAAGTCCAGA	RT-PCR, endogenous Rex1
Sox2-S1430	GGGAAATGGGAGGGGTGCAAAAGAGG	RT-PCR, endogenous Sox2
Sox2-AS1555	TTGCGTGAGTGTGGATGGGATTGGTG	RT-PCR, endogenous Sox2
Sox2-S691	GGCACCCCTGGCATGGCTCTTGGCTC	RT-PCR, exogenous Sox2
Oct3/4-S1165	GACAGGGGGAGGGGAGGAGCTAGG	RT-PCR, endogenous Oct3/4
Oct3/4-AS1283	CTTCCCTCCAACCAGTTGCCCCAAAC	RT-PCR, endogenous Oct3/4
Oct3/4-S944	CCCCAGGGCCCCATTTTGGTACC	RT-PCR, exogenous Oct3/4
Myc-S253	GCGTCCTGGGAAGGGAGATCCGGAGC	RT-PCR, endogenous Myc
Myc-AS555	TTGAGGGGCATCGTCGCGGGAGGCTG	RT-PCR, endogenous Myc
Myc-S1011	CAACAACCGAAAATGCACCAGCCCCAG	RT-PCR, exogenous Myc
Klf4-S1229-MY	CCCACACAGGTGAGAAACCTTACC	RT-PCR, endo/exogenous Klf4
Klf4-AS-MY	GTAGTGCTTTCTGGCTGGGCTC	RT-PCR, endogenous Klf4
pMXs-F1	CCTGAAATGACCCTGTGCCTTATTTG	nested PCR for viral integration
pMXs-F2	GTATCCAATAAACCCTCTTGCAGTTGC	nested PCR for viral integration
Sox2-R1	AGTGGGAGGAAGAGGTAACCAC	nested PCR for viral integration
Sox2-R2	CTGCGAGTAGGACATGCTGTAG	nested PCR for viral integration
Oct3/4-R1	CTCGAGCCCAAGCTGCTGG	nested PCR for viral integration
Oct3/4-R2	CGATGTGGCTGATCTGCTGCAG	nested PCR for viral integration
Myc-R1	CTTCTTGTTCCTCCTCAGAGTCGC	nested PCR for viral integration
Myc-R2	AGTCTTGCGAGGCGCAGGACTT	nested PCR for viral integration
Klf4-R1	CGGAATGTACACCGGGTCCAATTC	nested PCR for viral integration
Klf4-R2	GGACTCCCTGCCATAGAGGAG	nested PCR for viral integration
β-Actin-F	GCTCGTCGTCGACAACGGCTC	RT-PCR in iPSCs & cardiomyocytes
β-Actin-R	CAAACATGATCTGGGTCATCTTCTC	RT-PCR in iPSCs & cardiomyocytes
β-MHC-F	GACGGAGGAGGACAGGAAAAACCTGC	RT-PCR in cardiomyoctes
β-MHC-R	CAAAGCTACTCCTCATTCAAGCCCTTCGTG	RT-PCR in cardiomyoctes
ANP-F2	GAACCAGAGGGGAGAGACAGAGCAGC	RT-PCR in cardiomyoctes
ANP-R2	CCCTCAGCTTGCTTTTTAGGAGGGCAGATC	RT-PCR in cardiomyoctes
Cav1.2-exon7-F1-MY	GTTCCAGCAGAAGATGACCCTTCCCC	RT-PCR in cardiomyoctes
Cav1.2-exon8-R1-MY	GGGTAACTCATAGCCCATAGCGTCCTGC	RT-PCR in cardiomyoctes
Cav1.2-exon8a-F1-MY	GTCAATGATGCCGTAGGAAGGGACTGG	RT-PCR in cardiomyoctes
Cav1.2-exon9-R1-MY	GTTTCGGGGCTTCTCCTCATCCATGCC	RT-PCR in cardiomyoctes
MLC2v-F	CATGGACCAGAACAGGGATGGCTTCATTG	RT-PCR in cardiomyoctes
MLC2v-R	CCTCAGGGTCCGCTCCCTTAAGTTTC	RT-PCR in cardiomyoctes